Nonlinear polarization dynamics in directly modulated vertical-cavity surface-emitting lasers

M. Sciamanna,[1] A. Valle,[2] P. Mégret,[1] M. Blondel,[1] and K. Panajotov[3,*]
[1]*Service d'Electromagnétisme et de Télécommunications, Faculté Polytechnique de Mons, Boulevard Dolez 31, B-7000 Mons, Belgium*
[2]*Instituto de Fisica de Cantabria, Consejo Superior de Investigaciones Cientificas-Universidad de Cantabria, Facultad de Ciencias, Avenida Los Castros s/n, E-39005 Santander, Spain*
[3]*Department of Applied Physics and Photonics (TW-TONA), Vrije Universiteit Brussel, Pleinlaan 2, B-1050 Brussel, Belgium*
(Received 28 February 2003; published 11 July 2003)

A current-modulated vertical-cavity surface-emitting laser is shown to exhibit interesting nonlinear dynamics in its two orthogonal linearly polarized (LP), fundamental transverse modes. The intensities of the two LP modes may exhibit in-phase time-periodic dynamics or chaotic regimes with combination of in-phase and antiphase dynamics at two different time scales. Chaotic dynamics are found in a large range of laser and modulation parameters.

DOI: 10.1103/PhysRevE.68.016207 PACS number(s): 05.45.−a, 42.55.Px, 42.65.Sf

The dynamics of a semiconductor laser subject to direct current modulation has received a lot of attention, considering its potential to generate ultrafast sharp pulses but also its rich nonlinear behavior [1–5]. Most of existing studies relate, however, to conventional edge-emitting lasers (EELs). Studies of nonlinear dynamics in directly modulated vertical-cavity surface-emitting lasers (VCSELs) remain scarce [6,7] , while being of great interest both for fundamental and applied research [8]. Moreover, VCSELs are interesting devices considering their polarization properties and multiple transverse mode dynamics. Indeed VCSELs usually emit linearly polarized (LP) light along one of the two orthogonal directions (x and y), but may switch between these two LP eigenmodes due to the complex interplay of thermal effects [9–11], spatial hole burning [12], and nonlinear mechanisms [13,14]. High order transverse modes usually appear when VCSELs operate at large injection current [15]. These mode competitions may lead to a richer nonlinear dynamics in VCSELs than in EELs [16–19].

Previous studies on nonlinear dynamics in directly modulated VCSELs [6,7] have considered a VCSEL that is biased below the threshold and whose injection current is modulated with short pulses of very large amplitude (several times the threshold current) and high frequency (GHz). In that case, the VCSEL may experience strong transverse mode competition [20], which has been analyzed from the nonlinear dynamics viewpoint [6,7]. However, interesting dynamics is also expected to occur when the current-modulated VCSEL operates in the fundamental transverse regime (e.g., for smaller modulation amplitudes [20]), since it may still exhibit competition between the two LP modes. Gain difference between these LP modes is much smaller than gain differences between different transverse modes and then stronger mode competition is expected. To the best of our knowledge, the nonlinear dynamics of polarization modes in directly modulated VCSELs has not yet been studied, neither theoretically nor experimentally.

In this paper, we analyze the nonlinear dynamics of LP modes in VCSELs with direct current modulation, operating in a single, fundamental transverse mode. Different polarization dynamics are unveiled: the two LP modes may exhibit in phase pulsing at the modulation period or at one of its multiple, but chaotic regimes are also possible in which the two LP modes exhibit a combination of in-phase and antiphase dynamics at two different time scales. Chaotic regimes in the two LP modes are found in a large range of parameters. The reported polarization dynamics is robust against model variations and/or inclusion of spontaneous emission noise, hence motivating new experiments on VCSELs.

Our numerical study is based on the San Miguel, Feng, and Moloney (SFM) model [13,14], which has been largely used in comparison with experiments:

$$\dot{E}_{\pm} = \kappa(1+i\alpha)[(N\pm n)-1]E_{\pm} - (\gamma_a + i\gamma_p)E_{\mp} + \sqrt{\beta_{sp}(N\pm n)}\xi_{\pm}, \quad (1)$$

$$\dot{N} = -\gamma[N-\mu+(N+n)|E_+|^2+(N-n)|E_-|^2], \quad (2)$$

$$\dot{n} = -\gamma_s n - \gamma[(N+n)|E_+|^2-(N-n)|E_-|^2], \quad (3)$$

where $E_{\pm}$ are the left and right circularly polarized components of the slowly varying optical field. N is the total population difference between conduction and valence bands, n is the difference between the two distinct subpopulation inversion densities which couple separately to the emission of left and right circularly polarized light. κ is the field decay rate in the cavity, α is the phase-amplitude coupling factor, γ is the carrier relaxation rate. $\gamma_s \equiv \gamma + 2\gamma_j$, where γ_j is a coupling rate between the two circularly polarized radiation channels, which models different microscopic relaxation mechanisms that equilibrate the spin of carriers [13]. γ_p (γ_a) is the magnitude of linear birefringence (dichroism), per intracavity round-trip time. β_{sp} is the spontaneous emission rate and $\xi_{\pm}$ are Gaussian white noises of zero mean value and Δ correlated in time. μ is the normalized injection current ($\mu=1$ at threshold), modulated according to $\mu = \mu_{dc} + \Delta\mu\sin(2\pi F_u t)$, where μ_{dc} is the dc bias injection current, $\Delta\mu$ is the modulation amplitude, and $F_u \equiv 1/T_u$ is the modulation frequency. The injection current is clamped to $\mu=0$ when it becomes negative.

*Permanent address: Institute of Solid State Physics, 72 Tzarigradsko Chaussee Blvd., 1784 Sofia, Bulgaria.

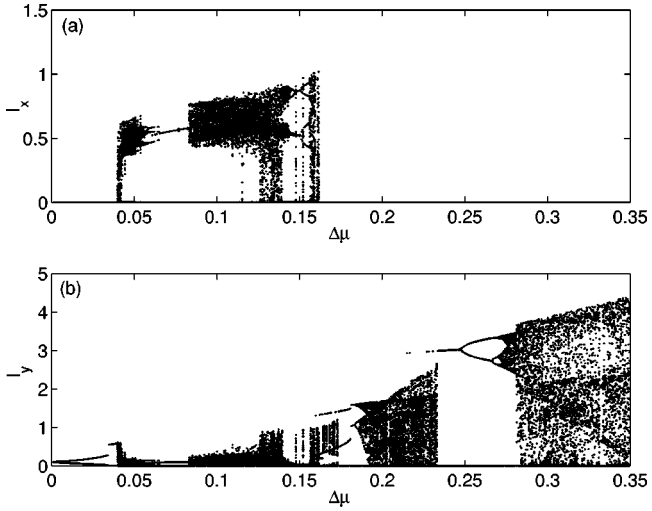

FIG. 1. Bifurcation diagrams of I_x (a), I_y (b) versus $\Delta\mu$, for $F_u=1$ GHz and the parameters specified in the text.

Figure 1 shows the bifurcation diagrams of LP mode intensities $I_{x,y}\equiv|E_{x,y}|^2$ as a function of $\Delta\mu$, for $F_u=1$ GHz and $\mu_{dc}=1.1$. Successive extrema of I_x and I_y are plotted. The laser parameters are $\gamma_a=0.1$ ns^{-1}, $\gamma_p=1$ ns^{-1}, $\gamma_s=50$ ns^{-1}, $\kappa=300$ ns^{-1}, $\alpha=3$, $\gamma=1$ ns^{-1}, and $\beta_{sp}=0$. F_u is smaller than the relaxation oscillation frequency of the VCSEL $F_{RO}\equiv\sqrt{2\kappa\gamma(\mu-1)}/2\pi=1.23$ GHz. For such parameters, the VCSEL under dc current operation emits only in the *y*-LP mode, because it is the only stable LP mode [14]. As $\Delta\mu$ increases, the VCSEL keeps on lasing in the *y*-LP mode, with its intensity sinusoidally modulated at the modulation period. For larger $\Delta\mu$, gain switching occurs as the injection current goes from below to above threshold current. Figure 1 shows ranges of $\Delta\mu$ in which the two LP modes coexist with chaotic or time-periodic dynamics. For still larger $\Delta\mu$, the VCSEL lases only in the *y*-LP mode with a period-doubling route to chaos.

The LP mode dynamics is further detailed in Fig. 2, which shows the time traces of I_x and I_y for specific values of $\Delta\mu$. At $\Delta\mu=0.04$ (a), the depressed *x*-LP mode is now lasing, i.e., direct current modulation has excited the LP mode that was depressed in the VCSEL under dc operation. The two LP modes exhibit chaoticlike dynamics with a fast modulation of their intensities at the modulation frequency complemented by a much slower envelope. Interestingly, the two LP modes emit in phase at the modulation frequency but the envelopes of their pulses are in partial antiphase: when one LP mode fires a large pulse, the other LP mode fires a small pulse. The partial antiphase dynamics is better seen in Fig. 2(b), which averages the dynamics of $I_{x,y}$ over the modulation period. For a slightly larger $\Delta\mu$ (c), the two LP modes exhibit a time-periodic pulsing at the modulation frequency. Moreover, the intensities of the two LP modes are in phase. For larger $\Delta\mu$, the *y*-LP mode is the only LP mode lasing. At $\Delta\mu=0.18$, it exhibits a period-3 time-periodic pulsing dynamics (d), followed by a chaotic dynamics (e). As we still increase $\Delta\mu$, the *y*-LP mode intensity follows a period-doubling route to chaos; see period 2 in (f).

Chaotic regimes in the two LP modes are found in a large range of modulation parameters. In Fig. 1, these chaotic regimes are found even for small $\Delta\mu$, i.e., a few percents of dc current. We also find such chaotic regimes for small modulation frequency. Figures 3(a) and 3(b) show the bifurcation diagrams of $I_{x,y}$ as a function of F_u, for $\Delta\mu=0.25$ and the same parameters as in Fig. 1. Regions of chaos in both LP modes are separated by windows of time-periodic dynamics in one or the two LP modes. Chaotic regimes, similar to that shown in Figs. 2(a) and 2(b), are found for F_u as small as a few hundreds of MHz.

The polarization dynamics of current-modulated VCSELs not only depends on modulation parameters but also on laser parameters such as γ_a, γ_p, γ_s, and α which define the polarization selection of VCSELs under dc operation [14]. Our objective in this paper is to illustrate typical dynamics, such as those of Fig. 2, often encountered in our numerical simulations. Besides the dynamics shown in Fig. 2, we find

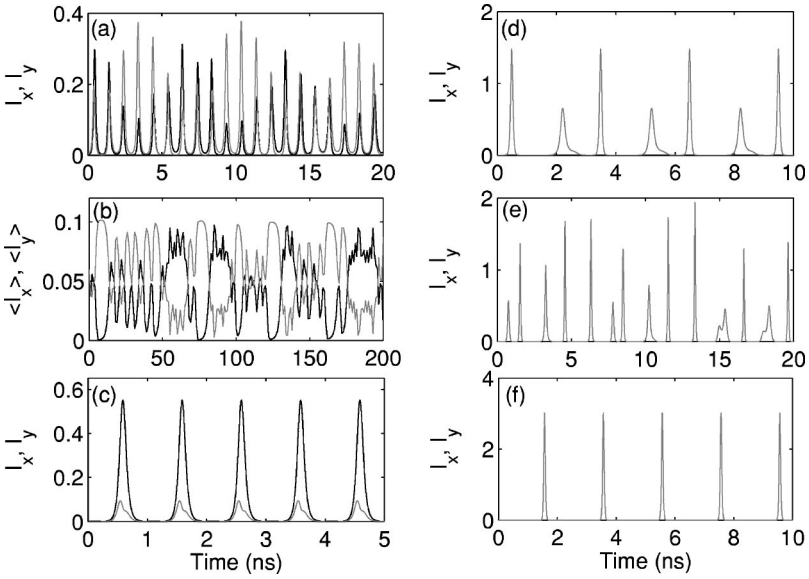

FIG. 2. Time traces of I_x (black) and I_y (gray) for specific values of $\Delta\mu$ in Fig. 1: (a) and (b) $\Delta\mu=0.04$, (c) $\Delta\mu=0.07$, (d) $\Delta\mu=0.18$, (e) $\Delta\mu=0.2$, (f) $\Delta\mu=0.24$. (b) is the same as (a) but averaged over 1 ns.

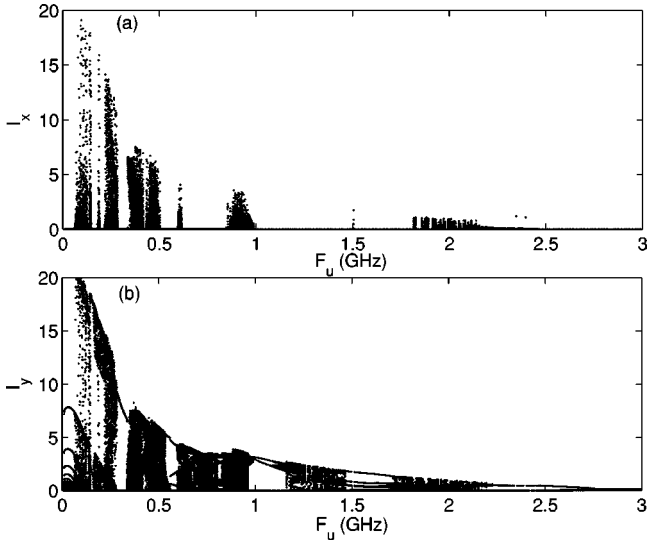

FIG. 3. Bifurcation diagrams of I_x (a), I_y (b) versus F_u, for $\Delta\mu = 0.25$ and the parameters specified in the text.

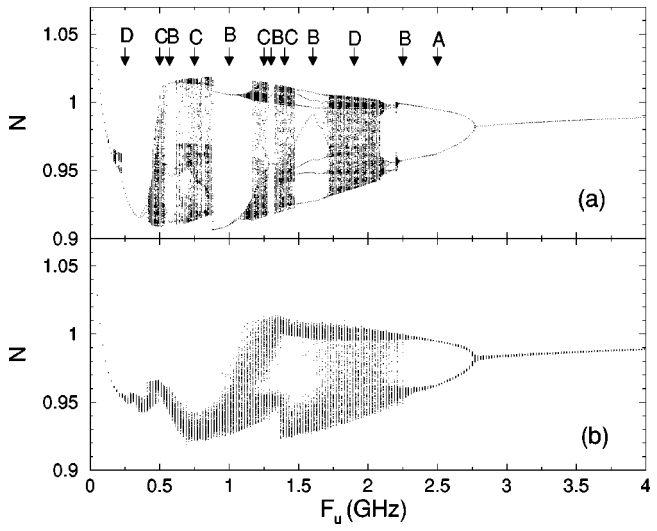

FIG. 5. Stroboscopic bifurcation diagram of N as a function of F_u, for the same parameters as in Fig. 3, with $\beta_{sp}=0$ (a) or $\beta_{sp}=10^{-5}$ ns^{-1} (b).

that the two LP modes may also coexist with a period-doubling dynamics leading to chaos. We find two types of period doubling in the two LP modes. In Figs. 4(a) and 4(b) are shown the time traces of I_x and I_y for the same parameters as in Fig. 1 but $F_u=5/3$ GHz, i.e., larger than F_{RO}. The two LP modes exhibit a period-doubling dynamics with an in-phase pulsing dynamics but in (b) the *y*-LP mode emits a pulse with a secondary peak in two modulation periods (period doubling of two periods [2,3]), while the *x*-LP mode in (a) exhibits a conventional period-doubling regime, i.e., emits a single pulse in two modulation periods. The LP modes exhibit, therefore, an asymmetry in their pulse shape. Another type of period doubling is shown in Figs. 4(c) and 4(d), which plot the time traces of $I_{x,y}$ for the same parameters as in Fig. 1 but $\mu_{dc}=1.4$. Each of the two LP modes exhibits what is called a period doubling of single period [3], i.e., the emission of two pulses at each modulation period. In contrast to the previous cases (a) and (b), the secondary peak is present in both LP modes. This last type of LP mode dynamics is more largely obtained when $F_u \leqslant F_{RO}$.

Chaos in the two LP modes is observed for a larger range of modulation amplitude and frequency as we decrease γ_s.

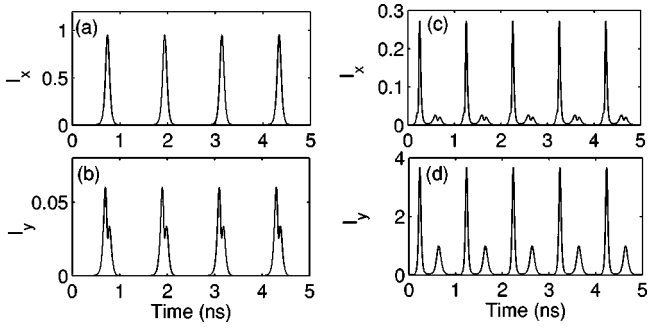

FIG. 4. Time traces of $I_{x,y}$ for the same parameters as in Fig. 1 and (a) and (b) $T_u=0.6$ ns, $\mu_{dc}=1.1$, $\Delta\mu=0.15$, or (c,d) $\mu_{dc}=1.4$, $T_u=1$ ns, $\Delta\mu=0.32$.

More specifically, if we fix the parameters to those of Fig. 1 but increase γ_s to more than 100 ns^{-1}, the VCSEL then shows a period-doubling route to chaos but lasing only in the *y*-LP mode. In contrast, both LP modes are excited in a large range of $\Delta\mu$ when decreasing γ_s towards its minimal value $\gamma_s=\gamma=1$ ns^{-1}. When γ_s is small, the fields $E_{\pm}$ indeed fail to phase lock to form stable LP modes [13,14]. This reduced stability in both LP modes then leads to a very wide region of chaotic regime in both LP modes. On the other hand, the regions of LP mode coexistence, which disappear when γ_s is large, may be recovered in a large range of modulation parameters if one decreases γ_a. Our results indicate, therefore, that nonlinear dynamics in the two LP modes can be obtained in a large range of γ_s, provided that one can vary γ_a. Experiments may benefit from reported techniques to modify linear anisotropies of the VCSEL cavity [21]. As a further confirmation of the robustness of our results, it is worth noting that we obtain qualitatively similar dynamics to those shown in Figs. 2 and 4 with a two-mode model, different from the SFM model, which does not include spin-relaxation processes [22,23].

Finally, we analyze the influence of spontaneous emission noise. We have plotted in Fig. 5 the bifurcation diagram of N as a function of F_u, for the same parameters as in Fig. 3, and either with $\beta_{sp}=0$ (a) or $\beta_{sp}=10^{-5}$ ns^{-1} (b). In contrast to Figs. 1 and 3 which plot the successive extrema of $I_{x,y}$, Fig. 5 shows the value of N at the end of each modulation period. This kind of ''stroboscopic'' diagram allows a clearer picture of the effect of the noise [5]. We may identify four qualitatively different behaviors; see labels in Fig. 5. In case *A* (for $F_u \geqslant 2.5$ GHz), noise has little effect, since the LP mode intensities do not switch to levels of the order of the noise level (around 10^{-4} or smaller). Case *B* corresponds to situations in which the *y*-LP mode only is lasing with a time-periodic dynamics in the deterministic case while the two LP modes are lasing in an erratic way in the stochastic case. Case *B* is illustrated in Fig. 6. As the *y*-LP mode exhibits gain switch-

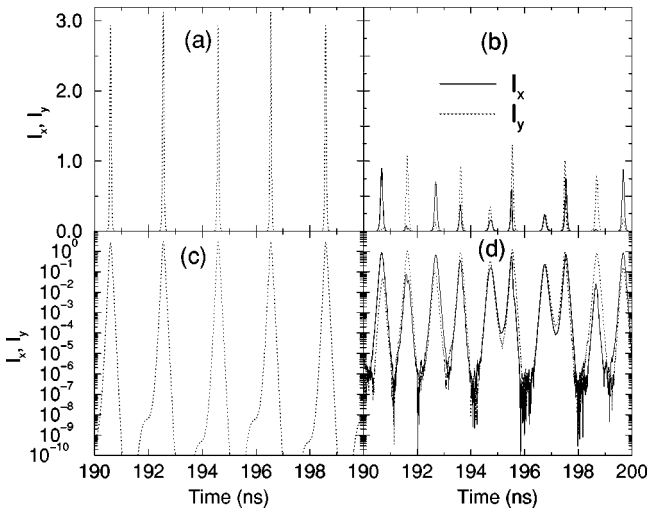

FIG. 6. Time traces of I_x (dashed line) and I_y (solid line) for the label *B* of Fig. 5, with $\beta_{sp}=0$ (a) or $\beta_{sp}=10^{-5}$ ns^{-1} (b). (c,d): same as (a) and (b) but in logarithmic scale.

ing, its intensity goes down to levels of the order of the noise level; see the logarithmic scale of Fig. 6. Noise then allows lasing in the other LP mode with non-negligible power. Excitation of one or the other polarization depends on the noise realization for each polarization. Case *C* is used for situations where the *y*-LP mode only is lasing in a chaotic way in the deterministic case while the two LP modes are lasing erratically in the stochastic case. As in *B*, intensities become comparable to the noise level and the two LP modes are then excited with non-negligible power. With the two modes excited, there can be less variation in *N* at the end of each modulation period than in the deterministic case, hence shrinking the bifurcation diagram of *N* as shown in Fig. 5(b). Finally, case *D* corresponds to situations where the two LP modes are lasing chaotically in the deterministic case. We discriminate between case *C* and case *B* by using the deterministic bifurcation diagram of $I_{x,y}$ in Fig. 3. With noise, the two LP modes in case *D* keep on lasing erratically. In all cases *B*–*D* in which the two LP modes are excited with noise and lase in an erratic way, the LP mode intensities exhibit a combination of fast in-phase pulsing and slow antiphase dynamics in the pulse envelopes [see Fig. 6(b)], as it is the case in the deterministic chaos of Figs. 2(a) and 2(b). Our results, therefore, suggest that this in-phase–antiphase combination would be largely observed experimentally.

In summary, we have shown that a directly modulated VCSEL may exhibit interesting nonlinear dynamics in its two orthogonal, fundamental transverse, LP modes. The LP mode intensities may exhibit in-phase time-periodic or period-doubling pulses. Chaotic regimes in the two LP modes are also found in a large range of laser and modulation parameters. In the chaotic dynamics, the LP mode intensities exhibit a combination of in-phase and antiphase dynamics at two different time scales, which is robust when including spontaneous emission noise.

M.S. was supported by FNRS (Belgium). Our research was supported by IAP V/18, the CICYT Project TIC2002-04255-C04-01, and Projects OCCULT (IST-2000-29683) and VISTA (HPRN-CT-2000-00034).

[1] C.H. Lee, T.-H. Yoon, and S.-Y. Shin, Appl. Phys. Lett. **46**, 95 (1985).
[2] Y.C. Chen, H.G. Winful, and J.M. Liu, Appl. Phys. Lett. **47**, 208 (1985).
[3] M. Tang and S. Wang, Appl. Phys. Lett. **48**, 900 (1986).
[4] H.-F. Liu and W.F. Ngai, IEEE J. Quantum Electron. **29**, 1668 (1993).
[5] K.A. Corbett and M.W. Hamilton, Phys. Rev. E **62**, 6487 (2000).
[6] J.Y. Law and G.P. Agrawal, Opt. Commun. **138**, 95 (1997).
[7] A. Valle, L. Pesquera, S.I. Turovets, and J.M. Lopez, Opt. Commun. **208**, 173 (2002).
[8] K. Iga, IEEE J. Sel. Top. Quantum Electron. **6**, 1201 (2000).
[9] K.D. Choquette, D.A. Richie, and R.E. Leibenguth, Appl. Phys. Lett. **64**, 2062 (1994).
[10] K. Panajotov, B. Ryvkin, J. Danckaert, M. Peeters, H. Thienpont, and I. Veretennicoff, IEEE Photonics Technol. Lett. **10**, 6 (1998).
[11] B. Ryvkin, K. Panajotov, A. Georgievski, J. Danckaert, M. Peeters, G. Verschaffelt, H. Thienpont, and I. Veretennicoff, J. Opt. Soc. Am. B **16**, 2106 (1999).
[12] A. Valle, L. Pesquera, and K.A. Shore, IEEE Photonics Technol. Lett. **9**, 557 (1997).
[13] M. San Miguel, Q. Feng, and J.V. Moloney, Phys. Rev. A **52**, 1728 (1995).
[14] J. Martin-Regalado, F. Prati, M. San Miguel, and N.B. Abraham, IEEE J. Quantum Electron. **33**, 765 (1997).
[15] C.J. Chang-Hasnain, J.P. Harbison, G. Hasnain, A. Von Lehmen, L.T. Florez, and N.G. Stoffel, IEEE J. Quantum Electron. **27**, 1402 (1991).
[16] A. Valle, L. Pesquera, and K.A. Shore, IEEE Photonics Technol. Lett. **10**, 639 (1998).
[17] H. Li, A. Hohl, A. Gavrielides, H. Hou, and K.D. Choquette, Appl. Phys. Lett. **72**, 2355 (1998).
[18] M. Sciamanna, T. Erneux, F. Rogister, O. Deparis, P. Mégret, and M. Blondel, Phys. Rev. A **65**, 041801(R) (2002).
[19] M. Sciamanna, C. Masoller, N.B. Abraham, F. Rogister, P. Mégret, and M. Blondel, J. Opt. Soc. Am. B **20**, 37 (2003).
[20] O. Buccafusca, J.L.A. Chilla, J.J. Rocca, S. Feld, C. Wilmsen, V. Mozorov, and R. Leibenguth, Appl. Phys. Lett. **68**, 590 (1996).
[21] K. Panajotov, B. Nagler, G. Verschaffelt, A. Georgievski, H. Thienpont, J. Danckaert, and I. Veretennicoff, Appl. Phys. Lett. **77**, 1790 (2000).
[22] Y.C. Chen and J.M. Liu, Appl. Phys. Lett. **46**, 16 (1985).
[23] M. Sciamanna, A. Valle, K. Panajotov, P. Mégret, and M. Blondel, Proc. SPIE (to be published).